POAC'13
Espoo, Finland

Proceedings of the 22nd International Conference on
Port and Ocean Engineering under Arctic Conditions
June 9-13, 2013
Espoo, Finland

CORRELATION CURVES FOR BRITTLE AND DUCTILE ICE FAILURE BASED ON FULL-SCALE DATA

Guido Kuiper,

Shell Global Solutions International B.V., THE NETHERLANDS

ABSTRACT

The global ice pressure exerted on the face of a structure is examined in this paper, based upon full-scale ice load data collected on the Molikpaq platform offshore the northeast coast of Sakhalin Island. It has been known for a while that when ice fails by crushing against a wide vertically-sided structure, it exhibits a scale effect - namely the average crushing pressure across an area reduces as the size of the loaded area increases.

The purpose of this paper is to assess the correlation coefficients between localized ice failure pressures across the face of a wide structure. Depending on the ice failure process, correlations over different distances and time scales are involved. Correlation curves are compared as obtained from the Molikpaq in Sakhalin, the Molikpaq in the Beaufort Sea and the medium-scale JOIA experiments. The results confirm that the interaction velocity, and hence the type of ice failure, has a strong influence on the distribution of ice load. Slow interactions result in ductile or creep failure. This type of interaction results in pressures that are more evenly spread than those involving brittle fracture, which occurs for larger ice drift speeds. As a result, the global ice load for ductile failure is higher due to the simultaneous pressure build-up over the complete face of the structure. Small-scale experiments have proven that the correlation is almost constant with distance during sustained ice-induced vibrations, i.e. during intermittent crushing and frequency lock-in.

The paper concludes with a design recommendation for brittle and ductile failure correlation curves. It is the author's opinion that the ISO 19906 global ice pressure equation requires modification to clearly visualize the dependency on the type of ice failure and the compliance of the structure.

1. PROBABILISTIC AVERAGING METHOD

A model based on a probabilistic approach to account for scale effect has been proposed by Jordaan, et al. (2005). The method is based on the assumption that ice crushing is the dominant failure mechanism and that the ice force is concentrated in localized zones, the so-called high-pressure zones (Jordaan, 2001). The pressures within these areas, where compressive forces are transmitted from the ice to the structure, fluctuate considerably both in space and time. The theory of ice failure mechanics suggests that the interaction velocity will have a strong influence on the distribution of the ice load. Slow interactions result in ductile failure leading to ice pressures that are evenly spread out. At higher ice velocities, the ice fails in a brittle way, leading to more pressure fluctuations. One expects that for brittle failure the average pressure over a wide structure will have significantly less variance than the pressure measured over a single panel, due to the probabilistic averaging effect.

This paper investigates whether the drop in correlation for different types of interaction is confirmed by full-scale measurements as obtained from the Molikpaq in the Sea of Okhotsk and in the Beaufort Sea.

2. ICE PRESSURE PANELS ON THE MOLIKPAQ

Jordaan's averaging method is evaluated by analysing the measured ice panel pressures on the Molikpaq caisson structure, located in the Beaufort Sea (1984-1990) and in the Sea of Okhotsk (from 1998 onwards). At both locations, the Molikpaq was equipped with an extensive instrumentation system consisting of pressure panels, strain gauges, extensometers, accelerometers, etc. The article by Frederking and Sudom (2006) describes the system as it was set-up in the Beaufort Sea.

For the deployment of the Molikpaq in the Beaufort Sea, the water depth was 31 m and the caisson was set down on a submarine berm, giving it a draft of 19.5 m. For this draft the caisson has near vertical sides (7^o from the vertical). In the Sea of Okhotsk the Molikpaq is located in nearly the same water depth, but resting on a 15 m high steel spacer rather than on a 19.5 high submarine berm. For this lower draft, the faces of the Molikpaq are sloped 23° from the vertical.

In this paper the focus is on the ice load panel pressure data. These panels have been fitted to the outside of the structure. The main advantage of the panels is the direct measurement of ice loading, in contrast to strain gauges and extensometers, which measure an averaged ice load indirectly.

2.1 Beaufort Sea

A total of 31 panels were installed on the north, northeast and east faces of the Molikpaq in the Beaufort Sea (Frederking and Sudom, 2006). Slightly more than 10% of the waterline length of each of the north and east faces were covered with panels. The panels were 1.135m wide and 2.715m high, with a capacity of 20 MN. The panels were clustered in groups of four or five.

There is still quite some hot dispute on the reliability of the pressure panels on the Molikpaq in the Beaufort Sea (e.g. Jordaan, et al., 2011 and Jefferies, et al., 2011). The main discussion point is the validity of the measured ice pressure due to potential softening of the polyurethane buttons. Since this paper focuses on correlation coefficients, the absolute magnitude of the pressure is less relevant.

2.2 Sea of Okhotsk

After the Molikpaq was purchased by the Sakhalin Energy Investment Company Ltd. (SEIC) in 1996 and modified for use in the Sakhalin II development project, new ice pressure panels were installed on the Molikpaq. An improvement of the panels at the Molikpaq in Sakhalin is the absence of polyurethane buttons, which avoids the debate on possible softening behaviour of the ice pressure panels. Eighteen ice load panels were installed on the north face. Each load panel is 2 m in height by 1 m in width and contains two pressure transducers that measure the loads on the panel's upper and lower sections. Hence, one pressure transducer provides ice load pressure data on 1 m x 1 m area. These panels have been placed in three separate groups near the west, centre, and east parts of the caisson's north face (termed N1, N2, and N3 – see Figure 1), where the most frequent ice loading events occur (due to predominant southward drift of ice). In the horizontal direction, adjacent panels are located at a distance of 1.299 m centre to centre, resulting in a small gap between the panels. In the vertical direction, a similar

gap between adjacent panels is present. The face of the Molikpaq is sloped 23° from the vertical and mean sea level passes through the middle of the top row of panels.

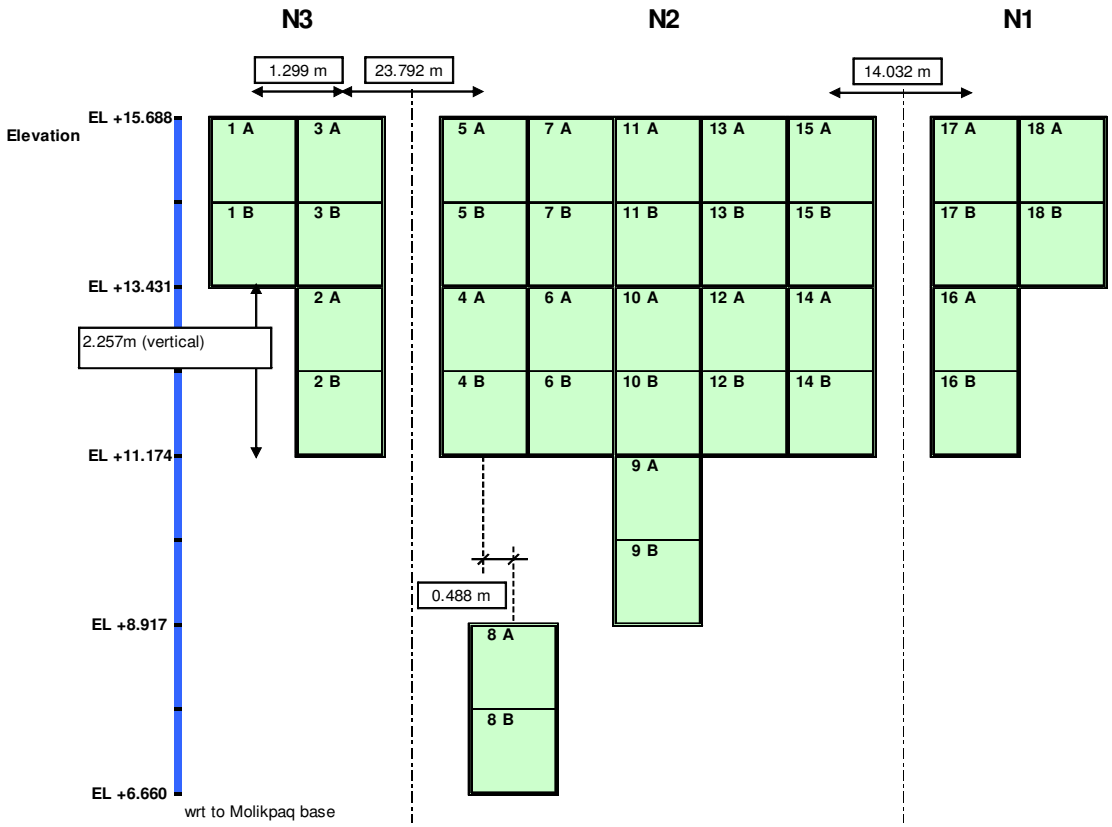

Figure 1: (Top) Ice load panels installed on the north face of the Molikpaq structure. **(Bottom)** Molikpaq during tow at a low draft. The three groups of pressure panels (N3, N2 and N1) are encircled.

Ice pressures are continuously sampled at a high scanning rate (75 Hz). Three different types of files have been generated from this 75 Hz data: burst, fast and slow files. All the analyses in this paper are based on the fast files. A fast file consists of instrument data which is stored at a rate of 1 Hz and records one measurement from the 75 Hz (scanned) data each second. Since significant variations in ice load levels on the Molikpaq usually occur over time scales that are in the order of a second or more, fast files provide good data sets for analyzing correlation between panels.

3. CORRELATION BETWEEN PANELS

The probabilistic averaging method considers that the ice pressures on adjacent areas of a platform are correlated over a certain length and that the degree of correlation drops off at larger distances. In this theory, ice loading has been represented by a Markov process in space, whereby the ice pressure on any panel is statistically correlated to adjacent panels.

In order to gain further insight on whether the probabilistic averaging method and the associated reductions in load are fully justified, a closer look at the Molikpaq data collected offshore Sakhalin was carried out. This data set offers the opportunity to test and validate Jordaan's model because of the increased number of panels in both the horizontal and vertical directions and the higher response time of the new ice load panels in comparison with the ice load panels in the Beaufort Sea.

In order to compute the correlation between panels, mathematical definitions are introduced (e.g. E. Vanmarcke, 1983). The standard deviation σ for an individual panel is determined by:

$$\sigma^2 = E\left[(X - m)^2\right] \tag{1}$$

where $E[..]$ is the expectation of the function, X is the ice pressure on one panel varying with time and m is the mean of the measured pressure. The correlation coefficient is related to two panels, X_1 and X_2. The dimensionless coefficient of correlation ρ_{12} between X_1 and X_2 is defined as:

$$\rho_{12} = \frac{E\left[(X_1 - m_1)(X_2 - m_2)\right]}{\sigma_1 \sigma_2} \tag{2}$$

It follows from the definition that $\rho_{12} = \rho_{21}$ and that ρ is bounded by –1 and 1. Two jointly distributed random variables are said to be perfectly correlated if $\rho = \pm 1$ and uncorrelated if $\rho = 0$.

The correlation coefficients between pairs of panels have been computed for all panels in the top row for a high loading event with a duration of 20 minutes sampled at 1 Hz. Figure 2 shows the correlation coefficients versus horizontal distance between the panels. For example, the most right circle at a horizontal distance of 45.6 m indicates the correlation coefficient between panels 1A and 18A (centre to centre 45.6 m in Figure 1). This low value of $\rho = 0.04$ indicates that there is no correlation over such a large distance. On the contrary, adjacent panels show a significant correlation ($\rho = 0.7$). Figure 2 shows a clear relation; the larger the horizontal distance between the panels, the lower the correlation coefficient.

Similar calculations have been performed for the second, third, and fourth row of panels. Although the same rate of reduction with distance is observed, the correlation coefficients are more scattered. The correlation in the vertical direction was also calculated, but appeared to be much smaller than in the horizontal direction. The reason for these lower and more scattered correlation coefficients seems to be the relatively thin level ice thickness in the Sakhalin area (mainly varying between 0.5 and 1.5 m). Therefore, significant ice pressures at deeper levels are mainly due to the presence of ridges. Based on the data, it appears that a

ridge rarely loads the entire face of the structure at the same time. This implies that at deeper, horizontal levels the loading is more fragmented (e.g., only a small part of the horizontal row is loaded by ice), and obviously, this results in more scatter in the correlation graph.

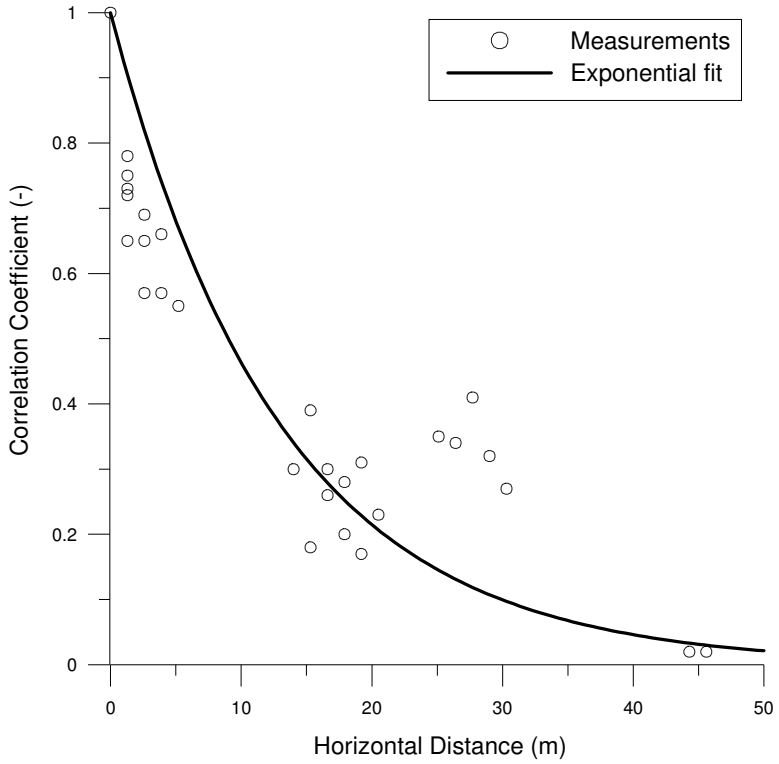

Figure 2: Correlation coefficient for pairs of panels in the top row as a function of horizontal distance.

To avoid these drawbacks, it was decided to compute the horizontal correlation coefficients based on column-averaged loads rather than on individual panel loads. Forces measured at individual panels in the same column are added, before the horizontal correlation coefficients are computed. The comparison is shown in Figure 3. The correlation coefficients based on column loads and individual panels have been indicated with black and red circles, respectively. For small horizontal distances both approaches give similar results. For horizontal distances over 20m the two approaches deviate. In this specific case, individual panels appear to be uncorrelated for distances exceeding 20m. In contrast to this, the column-based approach shows some correlation at larger distances. This implies that load transfer may not always be in one horizontal plane. To be on the conservative side, it seems better to use columns as a basic unit rather than individual panels and this approach is applied from here onwards.

There are several parameters which may influence the drop of correlation over distance. In the remaining part of the paper, the main parameter which is investigated is the ice failure mode, which is strongly linked to the ice drift speed.

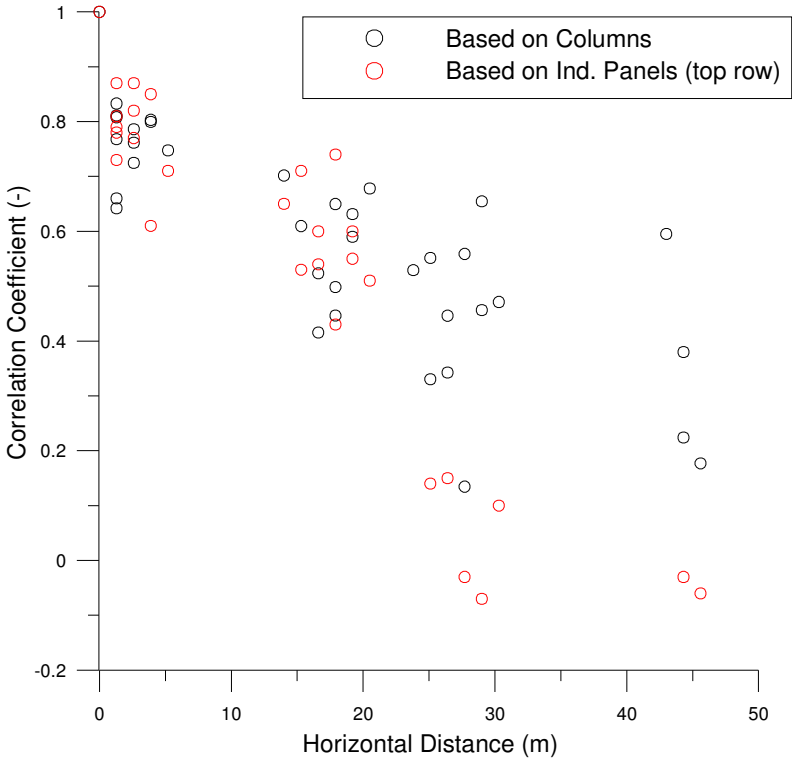

Figure 3: Correlation coefficient based on columns and based on individual panels (top row).

Nevertheless, the duration of an interaction event is another key parameter. This topic has been extensively studied by the author and deserves a dedicated paper which will be presented at a future POAC conference. Defining the event duration is not straightforward. Obviously, the peak loading should be part of the event, but whether to use an ice pressure threshold value, such as a pre-defined time window, or something else is a useful and interesting discussion. In this paper a more pragmatic approach is applied; the event duration is taken short enough to avoid the large influence of 'zero pressures' but at the same time long enough to avoid too few data points.

4. RESULTS FROM MOLIKPAQ OFFSHORE SAKHALIN

Analysis of the ice and ice load information collected on the Molikpaq in the Sea of Okhotsk showed that the primary ice failure mode was a mixed modal failure. These ice failures were highly non-simultaneous in space and time across the structure face and typically result in fairly low ice load levels. Time lapse video records showed only occasionally ice crushing events across large widths of the caisson, but these crushing events produced the highest loads.

Fast files are continuously available for the winters of 2003 and 2004. Unfortunately, for these winters, there is little information about the ice thickness or ice speed during major ice-structure interactions. Hence, it is not straightforward to examine possible relationships between ice thickness or ice speed and the dominant ice failure mode. This means that we are limited to the data gathered by the panel pressures, strain gauges and extensometers for inferring the ice mode failure. Based on the patterns in the ice load data during high load events, roughly three types of interaction events have been distinguished:

- Single Floe Impact. A floe impacts the caisson locally, resulting in large pressures at adjacent panels. Only a few panels are highly loaded for a period of typically 1-5 minutes.
- Sliding Floe. A floe impacts the caisson at a certain location. Floe movement with a mean direction not normal to the caisson face forces the floe to slide along the face of the structure. Adjacent panels show successively large pressure peaks.
- Large floe. A large ice sheet is pushed against a major part of the structure and as a result, many pressure panels are loaded. This kind of loading event can last for more than 15 minutes. It is inferred that crushing and rubbling occur during this interaction.

Many ice peak load events were studied and categorized under one of the three types of interaction events. For each ice failure type an upper-bound correlation curve was determined. Based on this work the following observations were made:

- Single floe impact and large floe crushing resulted in the highest correlation curves.
- As expected, less correlation was found during a sliding floe.
- The correlation coefficients obtained from ice crushing data showed more scatter.

5 INFLUENCE OF ICE DRIFT SPEED AND ICE FAILURE TYPE

In the Sea of Okhotsk, ice drift speeds are mostly in the range of 0.3 to 1.0 m/s with extremes up to 2.0 m/s. These fast ice drift speeds suggest that the ice crushing process will be governed by brittle fracture. The mechanics of ice failure (Jordaan, 2001) show that the interaction velocity will have a strong influence on the distribution of ice load. Slow interactions result in ductile or creep failure. The hypothesis is that this kind interaction will result in pressures that are more evenly spread out than those involving brittle fracture. To confirm this hypothesis, correlation curves for lower ice drift speeds are required. Some of the correlation curves obtained at the Molikpaq in the Beaufort Sea are quite useful, since the ice drift speeds in the Beaufort Sea are typically 0.05 – 0.1 m/s with a maximum up to 0.5 m/s. Hence, the correlation curves for very low speeds (<0.05 m/s) obtained at the Molikpaq in the Beaufort Sea (Frederking et. al., 2009) are compared to ones from larger ice drift speeds.

In the rest of this paper, correlation curves are compared for brittle and ductile failure as obtained from the Molikpaq in the Sea of Okhotsk (this paper), from the Molikpaq in the Beaufort Sea (Frederking et. al., 2009) and from the medium-scale JOIA experiments (Takeuchi et al., 2001).

In the JOIA (Japan Ocean Industries Association) project very systematic medium-scale measurements were performed in the harbour of Notoro Lagoon in Hokkaido, Japan using natural sea ice. The JOIA tests employed an indenter equipped with sensors (2112 in total) to measure local ice pressures and load cells on the actuators to measure the global ice force. The width of the indenter (0.6 m to 6 m), ice thickness (0.065 m to 0.451 m) and the indentation speed (0.03 cm/s to 3 cm/s) were varied as the main parameters influencing the total ice load and the ice failure mode in the test series (Takeuchi et al., 2001).

However, to compare correlation curves from medium-scale data with full-scale data one needs to correctly scale these curves. Takeuchi and co-workers (2001) as part of the JOIA project normalized the distance between panels by the ice thickness. The same approach is used here and gives remarkably good results. As shown by Takeuchi and co-workers (2004), the shape of ice pressure distribution along the ice thickness is quite different for brittle and ductile ice failure events.

To be able to normalize the correlation curves for the Beaufort Sea and Sea of Okhotsk an ice thickness had to be assumed due to the lack of specific measurements. Since the correlation curves are only obtained for high loading events, events with thicker ice were likely responsible for the obtained correlation curves. In this paper, ice thickness values of 1.5 m and 3.0 m are assumed for the Sea of Okhotsk and the Beaufort Sea, respectively.

5.1 Correlation curves for brittle failure against a rigid structure

For relatively high ice drift speed (exceeding ~0.2 m/s), the ice fails in a brittle manner. Based on the offshore Sakhalin measurements, an upper-bound correlation curve was obtained. The correlation curve was made dimensionless by using an ice thickness of 1.5 m:

$$\rho_{brittle,Sakhalin} = \exp\left(-\left(x/h\right)\cdot 0.06\right) \tag{3}$$

where x is the horizontal distance and h is the ice thickness. Since the ice speeds were not measured at the Molikpaq in the Sea of Okhotsk, the exact ice failure mode for each event is not known. However, due to the high currents in the Sea of Okhotsk brittle ice crushing is assumed to be the dominating failure mode for all events.

Based on the Molikpaq data from the Beaufort Sea (Frederking et al., 2009) a correlation curve was obtained for brittle failure by Jordaan. Video cameras and ice speed measurements in the Beaufort Sea made it possible to distinguish ductile and brittle ice failure events. Looking at only brittle ice failure events, and assuming an ice thickness of 3.0 m, the following non-dimensional correlation curve is obtained:

$$\rho_{brittle,Beaufort} = 0.68\left(1+\frac{x/h}{0.5}\right)\exp\left(-\frac{x/h}{0.5}\right)+0.32\left(1+\frac{x/h}{5}\right)\exp\left(-\frac{x/h}{5}\right) \tag{4}$$

The bi-functional expression was chosen to obtain the best fit through the data. To be able to use the JOIA data (Takeuchi et al., 2001), an upper-bound exponential function was fitted through the data points as measured during the medium-scale experiments where brittle fracture was observed (i.e. ice speed/ice thickness > 0.003 1/s):

$$\rho_{brittle,JOIA} = \exp\left(-\left(x/h\right)\cdot 0.4\right) \tag{5}$$

The three correlation curves as a function of dimensionless horizontal distance are compared in Figure 4. The curves from the Molikpaq in the Beaufort Sea and the JOIA data agree nicely. This is already an extremely interesting observation. By making the correlation curves dimensionless using the ice thickness, the curves are remarkably close while the structure dimensions vary over two orders of magnitude (0.6m versus ~60m).

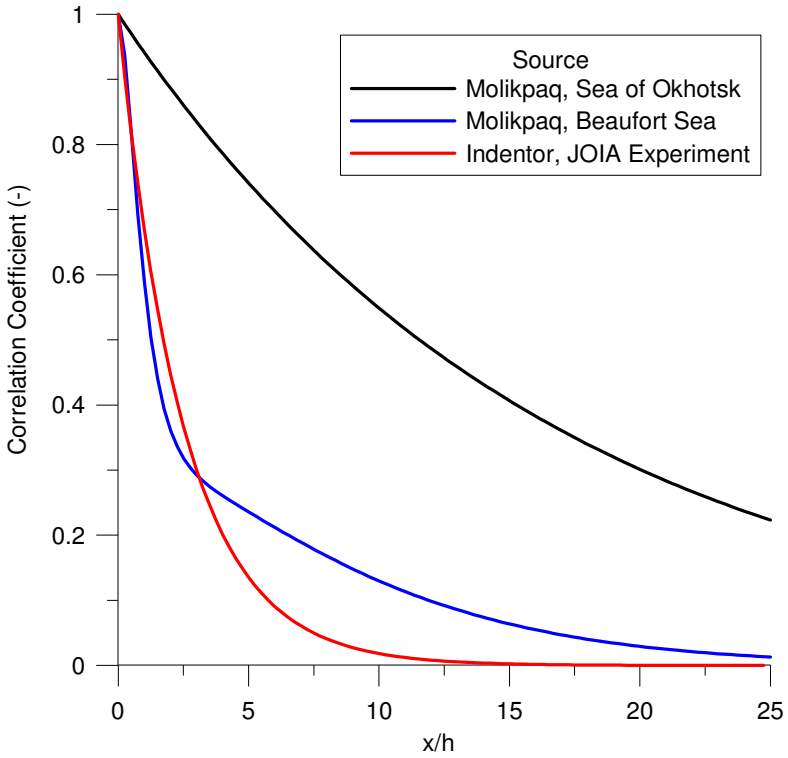

Figure 4: Medium-scale and large-scale correlation curves for *brittle* crushing failure.

The Sakhalin correlation curve is located slightly above the ones from the Beaufort Sea and JOIA data. As explained before, it is assumed that all ice crushing events in Sakhalin fail in a brittle manner. However, some of the high loading events may have occurred at low ice drift speeds leading to ductile failure. Hence, the higher correlation curve from Sakhalin may be caused by the fact that all ice events were not pure brittle failure.

5.2 Correlation curves for ductile failure against a rigid structure

Based on multiyear ice ductile events, as measured on the Molikpaq in the Beaufort Sea (Frederking et al., 2009) a bi-functional correlation function was recommended by Jordaan. This function is made dimensionless by assuming an ice thickness of 3.0 m:

$$\rho_{ductile,Beaufort} = 0.25(1 + x/h)\exp(-x/h) + 0.75\left(1 + \frac{x/h}{33}\right)\exp\left(-\frac{x/h}{33}\right) \quad (6)$$

A similar curve cannot be obtained from the Molikpaq data in the Sea of Okhotsk since it is assumed that the ice drift speed in this area is generally too high to create ductile crushing.

In the medium-scale JOIA experiments the indenter speed was also taken sufficiently low to observe ductile failure. An exponential function was fitted through the data points as measured during the ductile failure events (ice speed / ice thickness = 8.5×10^{-4}):

$$\rho_{ductile,JOIA} = \exp(-(x/h) \cdot 0.05) \quad (7)$$

These two curves for ductile failure are plotted in Figure 5. For the JOIA correlation curve, experimental data was only available for $x/h \leq 2$. Extrapolation and interpretation for larger

values should be taken with care. The Beaufort Sea ductile event corresponds reasonably well with the observations as found in the JOIA medium-scale ductile event, especially knowing that the values for the medium-scale ductile event exceeding x/h =2 are based on extrapolation and hence have more uncertainty.

Comparing Figures 4 and 5 it is clear that the ice failure type, and hence ice drift speed, has a crucial impact on the correlation curve. During brittle crushing events, the panel pressure responses are generally less correlated compared to those from a ductile failure. Due to the lower correlation, the global pressure for brittle events failure will be lower than for ductile events.

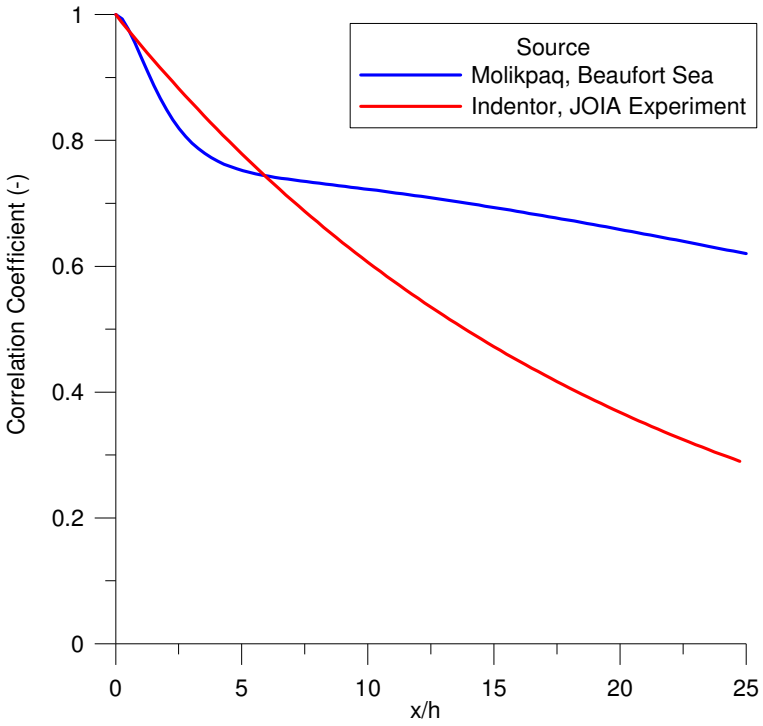

Figure 5: Medium-scale and large-scale correlation curves for *ductile* crushing failure.

5.3 Correlation curves for crushing against a compliant structure

The abovementioned correlation curves are only valid if the ice failure does not induce structural vibrations. Small-scale experiments have clearly shown that during ice-induced vibrations the loads on individual panels start to synchronize and ice failure occurs simultaneously along the width of compliant structures (Kamesaki et. al., 1996 and Sodhi, 1998). When simultaneous failure occurs, the correlation curve is close to 1, independent of the distance. Although the local ice pressure is not increasing, the global load increases due to the strong correlation.

A correlation curve of 1 is similar as assuming that there is no reduction in global ice pressure for increasing width of the structure. In this specific case, the equation for the global ice pressure should not be dependent on the structural width.

The author is not aware of correlation curves obtained from full-scale measurements when a wide structure was vibrating to prove that the correlation curve was close to 1. The Molikpaq in Sea of Okhotsk never experience sustained vibrations. The ice pressure panels on the Molikpaq were not functioning when the large loading event occurred in April 12, 1986 event

(Frederking and Sudom, 2006). However, it would be very interesting to check other vibration events on the Molikpaq in the Beaufort Sea like the May 12, 1986 event.

6. DISCUSSION AND CONCLUSIONS

In the past, medium-scale tests were carried out in order to obtain correlation curves for different ice speeds. However, it was unclear how the correlation curves obtained from medium-scale data could be correlated to full-scale data. In the previous sections, it was demonstrated that the ice thickness seems to be a good parameter to normalize the horizontal distance. For design the following curves are recommended, based on the most conservative correlation curve:

- Ductile failure against a rigid structure:

$$\rho_{ductile} = 0.25(1 + x/h)\exp(-x/h) + 0.75\left(1 + \frac{x/h}{33}\right)\exp\left(-\frac{x/h}{33}\right) \quad (8)$$

- Brittle failure against a rigid structure:

$$\rho_{brittle} = \exp\left(-(x/h)\cdot 0.06\right) \quad (9)$$

- Crushing against a compliant structure:

$$\rho_{compliant} = 1.0 \quad (10)$$

ISO 19906 provides an equation to calculate the global effective pressure. The global effective pressure is used in combination with ice thickness and structural width to calculate global ice actions:

$$p_G = C_R\left(\frac{h}{h^*}\right)^n\left(\frac{w}{h}\right)^m \quad (11)$$

in which p_G is the global average pressure, w is the width of the structure, h is the thickness of the ice sheet, h^* is a reference ice thickness of 1 m, C_R is the ice strength coefficient and m and n are empirical exponents (m= -0.16 and n = -0.30 for $h \geq 1.0$m). Eq. 11 can be rewritten in the following form:

$$p_G = C_R(wh)^{n/2}\left(\frac{w}{h}\right)^{m-n/2} \quad (12)$$

After substituting the numerical values for the coefficients n and m (assuming h ≥ 1.0m), Eq. 12 can be approximated by:

$$p_G = C_R(wh)^{-0.15}\left(\frac{w}{h}\right)^{-0.01} \approx C_R(wh)^{-0.15} \quad (13)$$

The approximation at the right hand side is valid for aspect ratios up to 200 (nearly all ice-structure events will fall in this range). This last equation demonstrates that the global ice pressure in ISO 19906 is described as a function of the structural width to the power -0.15. This raises the question whether the power -0.15 may produce too much reduction in global ice pressure for structures which may experience sustained vibrations. This paper shows that for compliant structures where phase-locked loading events may occur, i.e. the ice will fail simultaneously along the width of the structure, the correlation curve of 1.0 is recommended and no reduction in ice load occurs.

On the other hand, for ductile failure and, even more pronounced, for brittle failure the power -0.15 may be overly conservative, based on the presented correlation curves from full-scale data.

The author is of the opinion that the global pressure equation in ISO (Eq. 11) needs to be revisited to reflect the effect of the ice failure type (ductile or brittle) and to reflect the compliance of the structure (rigid or compliant).

REFERENCES

Frederking, R. and Sudom, D., Maximum ice force on the Molikpaq during the April 12, 1986 event, Cold Regions Science and Technology 46 (3), pp. 147-166, 2006.

Frederking, R., Sudom, D., Bruce, J., Fuglem, M., Jordaan, I., Hewitt, K., Analysis of multi-year ice loads, Molikpaq data (1985-86 winter deployment), 2009.

Jefferies, M., Rogers, B., Hardy, M., and Wright, B., Ice load measurements on Molikpaq: Methodology and Accuracy, POAC11-189, 2011.

Jordaan, I.J., Mechanics of ice-structure interaction, Engineering Fracture Mechanics 68, pp. 1923-1960, 2001.

Jordaan, I.J., Li, C., Mackey, T., et al., Design ice pressure-area relationships; Molikpaq data, PERD/CHC Report 14-121, Memorial University of Newfoundland, 2005.

Jordaan, I.J., Bruce, J., Hewitt, K. And Frederking, R., Re-evaluation of ice loads and pressures measured in 1986 on the Molikpaq structure, POAC11-130, 2011.

Kamesaki, K., Yamauchi, Y. and Kärnä, T., Ice force as a function of structural compliance, Proc. 13th IAHR, Ice Symposium, Beijing, Vol. I, pp 395-402, 1996.

Sodhi, D.S., Nonsimultaneous crushing during edge indentation of freshwater ice sheets, Cold Regions Science and Technology 27, pp. 175-195, 1998.

Takeuchi, T., Sakai, M., Akagawa, S., Nakazawa, N. and Saeki, H., On the factors influencing the scaling of ice forces, IUTAM Symposium in scaling laws in ice mechanics and ice dynamics, 2001.

Takeuchi, T., Akagawa, S., Nakazawa, N., Kioka, S. and Saeki, H., Local ice pressure distribution acting on offshore structure, IAHR conference proceeding, 2004.

Vanmarcke, E., Random Fields: Analysis and Synthesis, The MIT Press, Cambridge, Massachusetts, London, England, 1983.